H-Φ Field Formulation with Lumped Sources and Unbounded Domains

D. Casati and J. Smajic and R. Hiptmair

___

H-Φ Field Formulation
with Lumped Sources and Unbounded Domains

Daniele Casati[1], Jasmin Smajic[2], *Member, IEEE*, and Ralf Hiptmair[1]

[1]Seminar for Applied Mathematics, ETH Zurich, Switzerland, daniele.casati@sam.math.ethz.ch
[2]Institute for Energy Technology, Hochschule für Technik Rapperswil, Switzerland, jasmin.smajic@hsr.ch

We consider a H-Φ field formulation to solve 3D frequency-domain eddy-current problems. This formulation uses vector and scalar tetrahedral finite elements within, respectively, the conductive and nonconductive domain. It can handle multiply-connected regions and eliminates the need to compute the source current density and magnetic field before the actual simulation.

We propose three ways to couple finite elements with the Multiple Multipole Program (MMP) and solve this H-Φ variational form on an unbounded domain. MMP is a method that uses exact solutions of the homogeneous equations as basis functions (the so-called "multipoles"). The desired behavior at infinity is given by the chosen multipoles: this eliminates the need of artificially truncating the computational domain. Interface conditions between the FEM and MMP domains allow to express the coupled FEM–MMP problem.

Index Terms—Maxwell equations, Electromagnetic analysis, Finite element analysis, Numerical simulation.

I. INTRODUCTION

Two major numerical methods for magnetostatics and eddy currents have already been identified in the '70s: the $\mathbf{A}$-$\mathbf{A}$ and $\mathbf{T}$-Ω methods [1]. The $\mathbf{A}$-$\mathbf{A}$ approach employs a magnetic vector potential ($\mathbf{A}$) in both the electrically conductive (Ω_c) and nonconductive (Ω_n) domains. The $\mathbf{T}$-Ω approach employs an electric vector potential ($\mathbf{T}$) in conductive domains and a magnetic scalar potential (Ω) elsewhere.

The $\mathbf{H}$-Φ formulation was suggested as an alternative to the $\mathbf{T}$-Ω method [2]. Working with the $\mathbf{H}$-field in conductors and a magnetic scalar potential (Φ) in nonconductors, this method typically requires the source magnetic field ($\mathbf{H}_s$) and has difficulties with multiply-connected domains.

[3] proposes a new $\mathbf{H}$-Φ field formulation on a multiply-connected domain not requiring to precompute the $\mathbf{H}_s$-field before the actual simulation. Here we present another formulation with the same property: we solve it on an unbounded domain by coupling finite elements with basis functions that are exact solutions of the homogeneous equations.

II. BOUNDARY VALUE PROBLEM

We consider the same boundary value problem for eddy currents as in [3], but on an unbounded domain Ω_n. Boundary conditions are only imposed on symmetry planes.

$$
\begin{cases}
\nabla \times \left(\sigma_c^{-1} \nabla \times \mathbf{H}_c \right) + \imath\omega\mu_c\,\mathbf{H}_c = \mathbf{0} & \text{in } \Omega_c \\
\mathbf{n} \times \nabla \times \mathbf{H}_c = \mathbf{0} & \text{on } \partial_N\Omega_c \\
\mathbf{n} \times \mathbf{H}_c = \mathbf{0} & \text{on } \partial_D\Omega_c \\
\mathbf{H}_n = \nabla\Phi_n,\ \ \nabla \cdot (\mu_n\nabla\Phi_n) = 0 & \text{in } \Omega_n \\
\mathbf{n} \cdot \nabla\Phi_n = 0 & \text{on } \partial_N\Omega_n \\
\Phi_n = I/2 & \text{on } \partial_{D1}\Omega_n \\
\Phi_n = 0 & \text{on } \partial_{D2}\Omega_n \\
\Phi_n \text{ is const} & \text{on } \partial_{D3}\Omega_n
\end{cases}
\tag{1}
$$

Φ_n on $\partial_{D3}\Omega_n$ is a constant potential that has to be determined. The following behavior at infinity completes the problem:

$$
\Phi_n(\mathbf{x}) = \mathcal{O}\left(\|\mathbf{x}\|^{-1} \right) \quad \text{for } \|\mathbf{x}\| \to \infty .
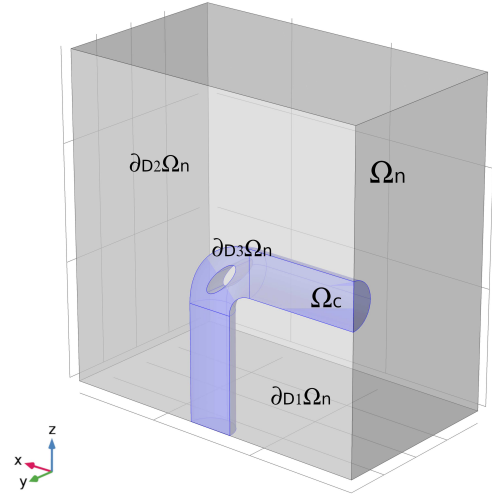\tag{2}
$$

Fig. 1. Domains Ω_c (one octant of a holed wire) and Ω_n (surrounding unbounded box). $\partial_D\Omega$ is the intersection with the XZ-plane (frontal face of the figure). $\partial_N\Omega$ comprises the boundaries that intersect the YZ- and XY-planes (right and bottom face, respectively). All other boundaries of the figure are fictitious: Ω_n extends to infinity.

Figure 1 illustrates the multiply-connected domain Ω_c and (a part of) Ω_n. Interface conditions between Ω_c and Ω_n are then required for the field to be well-posed:

$$
\begin{cases}
\mu_c\,\mathbf{n} \cdot \mathbf{H}_c = \mu_n\,\mathbf{n} \cdot \nabla\Phi_n \\
\mathbf{n} \times \mathbf{H}_c = \mathbf{n} \times \nabla\Phi_n
\end{cases}
\quad \text{on } \partial_{cn}\Omega_c .
\tag{3}
$$

III. COUPLING FINITE ELEMENTS AND AUXILIARY SOURCES

We propose to solve electromagnetic problems on unbounded domains using two numerical techniques in different subdomains that share a boundary: the *Finite Element Method* (FEM) and the *Multiple Multipole Program* (MMP). MMP belongs to the class of methods of auxiliary sources and has

successfully been applied to computational electromagnetics for many years [4].

FEM and MMP enjoy complementary capabilities.

FEM requires a mesh of the computational domain of interest. This is expensive, but can treat inhomogeneous materials or complicated geometries. Moreover, FEM employs basis functions with a finite support, allowing a purely local construction of the discrete system of equations.

Conversely, MMP uses global basis functions with central singularities that solve the homogeneous equations exactly and are placed outside the domain of approximation (the *multipoles*): their coefficients are established by imposing boundary conditions on hypersurfaces. The obtained linear combination is valid in the whole domain where the equations hold, which can be unbounded. MMP performs well where the electromagnetic field is easy to model, i.e. in the free space far from physical sources and material interfaces.

Thus, a natural way to combine the strengths of these methods arises when one needs to simulate the electromagnetic field of complicated structures surrounded by free space: use FEM on a mesh defined on the structures and MMP in the unbounded complement. The boundary between the FEM and MMP domains can be artificial if one surrounds the structures by a conforming mesh of an "air box", also modeled by FEM.

The proposed coupling offers computational advantages. For FEM, there is no need to approximate the field by imposing a boundary condition on the mesh. For MMP, the approximation is rather robust with respect to the locations of the centers of multipoles if an artificial FEM–MMP boundary is used.

The interface conditions between the FEM and MMP domains are key to accurate coupled FEM–MMP solutions. In [5], [6] for Poisson's equation and [7] for magnetostatic Maxwell's equations, different ways to achieve this coupling are explored. An approach (*Dirichlet-to-Neumann-based coupling*) imposes interface conditions through the boundary terms arising from the variational form of FEM, except one, which is enforced weakly with multipoles as test functions. Two other approaches are based on the mortar element method (*multi-field coupling*) and Discontinuous Galerkin (*DG-based coupling*).

IV. $\mathbf{H}$-Φ FIELD FORMULATION

Given the boundary value problem (1), we treat all the boundaries that do not intersect symmetry planes in Fig. 1 as artificial boundaries where we impose the coupling between FEM and MMP.

Considering the variational form found in [8, p. 19, Problem DHP], we aim at minimizing the functional

$$J_{\Omega^f}(\mathbf{H}_c^f, \Phi_n^f) := \int_{\Omega_c^f} \sigma_c^{-1} \left(\nabla \times \mathbf{H}_c^f\right) \cdot \left(\nabla \times \mathbf{H}_c^f\right) d\mathbf{x} +$$

$$\imath\omega \int_{\Omega_c^f} \mu_c \, \mathbf{H}_c^f \cdot \mathbf{H}_c^f \, d\mathbf{x} + \imath\omega \int_{\Omega_n^f} \mu_n \, \nabla \Phi_n^f \cdot \nabla \Phi_n^f \, d\mathbf{x} \quad (4)$$

subject to

$$\mathbf{n} \times \mathbf{H}_c^f = \mathbf{n} \times \nabla \Phi_n^f \qquad \text{on } \partial_{cn}\Omega^f \quad (5)$$

and

$$\begin{cases} \mathbf{n} \cdot \nabla \Phi_n^f = \mathbf{n} \cdot \nabla \Phi_n^m \\ \Phi_n^f = \Phi_n^m \end{cases} \quad \text{on } \partial_{fm}\Omega^f. \quad (6)$$

Superscripts f and m in the equations stand for FEM and MMP, respectively. Note that σ_c, μ_c, μ_n can be local parameters in Ω^f, but μ_n needs to be constant in $\Omega^m := \mathbb{R}^3 \setminus \Omega^f$.

As discretization, we take a mesh of tetrahedrons $\mathcal{M}$ on $\Omega^f := \Omega_c^f \cup \Omega_n^f$ and approximate $\mathbf{H}_c^f \in \mathbf{H}(\mathbf{curl}, \Omega_c^f)$ with the first family of lowest-order Nédélec edge elements, i.e. $\mathbf{V}_h = \mathcal{R}^1(\mathcal{M}_f)$, and $\Phi_n^f \in H^1(\Omega_n^f)$ with piecewise-linear Lagrangian finite elements, i.e. $V_h = \mathcal{S}_1^0(\mathcal{M}_f)$. Dirichlet boundary conditions in (1) are imposed strongly by setting the affected degrees of freedom of $\mathbf{V}_h, V_h$ accordingly.

Outside Ω^f, multipoles that respect (1) and (2) have the form

$$\Phi_n^m(r, \theta, \varphi) = r^{-(l+1)} Y_{lm}(\theta, \varphi),$$
$$l = 0, \ldots, \infty, \qquad m = -l, \ldots, l, \quad (7)$$

where Y_{lm} are complex spherical harmonics and the origin of Φ_n^m is shifted inside the volume of Fig. 1. To form a multipole, in addition to (7), there are seven other terms whose origins are symmetrically disposed such that the boundary conditions of (1) are respected on the infinite symmetry planes of Ω_n ($\partial_N\Omega_n$ and $\partial_{D2}\Omega_n$). We call the discrete space of chosen multipoles $\mathcal{T}_h(\Omega^m)$.

Equation (5) is then imposed by (scalar) Lagrange multipliers for each edge ℓ of $\mathcal{M}$ on $\partial_{cn}\Omega^f$, relying on the identity

$$\int_{\ell_i} \mathbf{t} \cdot \mathbf{v}_i \, d\vec{s} = v_{i1}(\mathbf{x}_{i1}) - v_{i2}(\mathbf{x}_{i2}), \quad i = 1, \ldots, N_{edges}^{bnd}, \quad (8)$$

with $\mathbf{v}_i \in \mathbf{V}_h$, $v_{i1}, v_{i2} \in V_h$, and $\mathbf{x}_{i1}, \mathbf{x}_{i2}$ corners of edge ℓ_i. The other interface condition in (3) is imposed implicitly.

The way the interface conditions in (6) are considered leads to different FEM–MMP coupling approaches [6], [7].

V. COUPLING STRATEGIES

The FEM–MMP coupling is done on the artifical interface $\Gamma := \partial_{fm}\Omega^f$ inside Ω_n. Hence, in the description we drop the subscript n when unnecessary and omit the (purely FEM) terms of (4) expressing the problem in Ω_c. We also define the Neumann trace operator $\gamma : H^1(\nabla^2, \Omega_n) \to H^{-\frac{1}{2}}(\Gamma)$, $\gamma\phi := \mu_n \mathbf{n} \cdot \nabla \phi$ for any $\phi \in H^1(\nabla^2, \Omega_n)$.

A. Dirichlet-to-Neumann-based Coupling

This coupling approach is the special case of the *Trefftz co-chain calculus* presented in [9]. The second interface condition in (6) is imposed in weak form by testing it with $\gamma\phi^m$, given $\phi^m \in \mathcal{T}(\Omega^m)$:

$$\int_{\Gamma} \left(\Phi^f - \Phi^m\right) \gamma\phi^m \, dS = 0 \quad \forall \phi^m \in \mathcal{T}(\Omega^m). \quad (9)$$

Combining (9) with the variational form of FEM in Ω_n^f, we end up with the following symmetric system:

$$\begin{aligned} &\text{Seek } \Phi^f \in H^1(\Omega_n^f), \ \Phi^m \in \mathcal{T}(\Omega^m): \\ &\begin{cases} \int_{\Omega_n^f} \left(\mu_c \nabla \Phi^f \cdot \nabla \phi^f\right) d\mathbf{x} - \int_{\Gamma} \gamma\Phi^m \phi^f \, dS = 0 \\ -\int_{\Gamma} \Phi^f \gamma\phi^m \, dS + \int_{\Gamma} \Phi^m \gamma\phi^m \, dS = 0 \\ \forall \phi^f \in H^1(\Omega_n^f), \forall \phi^m \in \mathcal{T}(\Omega^m), \end{cases} \end{aligned} \quad (10)$$

where the bottom-right term is symmetric because of $\Phi^{\mathrm{m}}, \phi^{\mathrm{m}} \in \mathcal{T}(\Omega^{\mathrm{m}})$.

B. Multi-Field Coupling

Mortar element methods allow to use FEM with nonconforming meshes on different neighboring domains for the same boundary value problem [10]. This is well-suited for the coupling because one can think of MMP as FEM with special functions acting on a "mesh with a single cell" defined on Ω^{m}.

With the same idea, the multi-field coupling approach imposes the second continuity (6) in a weak sense, like (9), by means of a Lagrange multiplier $\lambda \coloneqq \gamma \phi^{\mathrm{m}}$. Note that the continuity we want to impose connects traces in $H^{\frac{1}{2}}(\Gamma)$, and therefore λ has to belong to the dual space $H^{-\frac{1}{2}}(\Gamma)$.

Hence, the multi-field coupling can be expressed by the following Lagrangian:

$$\mathrm{L}(\Phi^{\mathrm{f}}, \Phi^{\mathrm{m}}, \lambda) \coloneqq \mathrm{J}_{\Omega_{\mathrm{n}}^{\mathrm{f}}}(\Phi^{\mathrm{f}}) + \mathrm{J}_{\Omega^{\mathrm{m}}}(\Phi^{\mathrm{m}}) + \int_{\Gamma} \left(\Phi^{\mathrm{f}} - \Phi^{\mathrm{m}} \right) \lambda \, \mathrm{d}S. \tag{11}$$

The functional $\mathrm{J}_{\Omega_{\mathrm{n}}^{\mathrm{f}}}(\Phi^{\mathrm{f}}) \coloneqq \int_{\Omega_{\mathrm{n}}^{\mathrm{f}}} \mu_{\mathrm{n}} \|\nabla \Phi^{\mathrm{f}}\|_{\ell^2}^2 \, \mathrm{d}\mathbf{x}$ is the term of (4) that expresses the problem in $\Omega_{\mathrm{n}}^{\mathrm{f}}$, while $\mathrm{J}_{\Omega^{\mathrm{m}}}$ has the same formulation, but can be rewritten as a boundary integral:

$$\mathrm{J}_{\Omega^{\mathrm{m}}}(\Phi^{\mathrm{m}}) \coloneqq \int_{\Omega^{\mathrm{m}}} \mu_{\mathrm{n}} \|\nabla \Phi^{\mathrm{m}}\|_{\ell^2}^2 \, \mathrm{d}\mathbf{x} = \int_{\Gamma} \gamma \Phi^{\mathrm{m}} \, \Phi^{\mathrm{m}} \, \mathrm{d}S. \tag{12}$$

The discretization of $\lambda \in H^{-\frac{1}{2}}(\Gamma)$ is a topic debated in the literature [11, Section 4]: in the spirit of mortar element methods, we opt for the Dirichlet traces of the finite elements in V_h, which discretizes one of the neighboring domains [11, p. B426].

C. Discontinuous Galerkin

As for the multi-field coupling, we again treat the MMP discretization as a finite element with special functions. Here we exploit the other main approach for imposing weak continuity on nonconforming meshes, which is the *Discontinuous Galerkin* (DG) method [12].

Under this idea, the coupling can be expressed as a *discrete* minimization problem for the following Lagrangian:

$$\mathrm{L}(\Phi_h^{\mathrm{f}}, \Phi_h^{\mathrm{m}}) \coloneqq \mathrm{J}_{\Omega_{\mathrm{n}}^{\mathrm{f}}}(\Phi_h^{\mathrm{f}}) + \mathrm{J}_{\Omega^{\mathrm{m}}}(\Phi_h^{\mathrm{m}}) +$$
$$\int_{\Gamma} \left(\Phi_h^{\mathrm{f}} - \Phi_h^{\mathrm{m}} \right) \mathrm{P}_h (\Phi_h^{\mathrm{f}} - \Phi_h^{\mathrm{m}}) \, \mathrm{d}S, \tag{13}$$

where $\mathrm{J}_{\Omega_{\mathrm{n}}^{\mathrm{f}}}$ and $\mathrm{J}_{\Omega^{\mathrm{m}}}$ are the same as for the multi-field coupling.

Depending on the choice of the discrete operator $\mathrm{P}_h : H^{\frac{1}{2}}(\Gamma) \to H^{-\frac{1}{2}}(\Gamma)$, we obtain different DG approaches. We follow the *Interior Penalty DG method* [13]:

$$\mathrm{P}_h(\phi) \coloneqq \epsilon_{\mathbf{n}} \, \gamma \phi + \eta \, \phi. \tag{14}$$

- $\epsilon_{\mathbf{n}}(\mathbf{x}) : \mathbb{R}^3 \to \{1, -1\}$ is $= 1$ if one is integrating on Γ from the side of $\Omega_{\mathrm{n}}^{\mathrm{f}}$ and $= -1$ from the side of Ω^{m}.
- $\eta \in \mathbb{R}$ is a penalty parameter that needs to be assigned heuristically and should be proportional to N^{m}/h, where N^{m} is the number of degrees of freedom of $\mathcal{T}_h(\Omega^{\mathrm{m}})$ and $h \in \mathbb{R}$ the meshwidth of $\mathcal{M}$ restricted to Γ.

VI. Implementation

Meshes were generated using `Comsol`.

Our code is written in `C++14`, using `C++11` multithreading for parallelization. We use `Eigen` v3.3.7 for linear algebra and `HyDi` [14] for the FEM component. The `PARDISO` v6.0 solver provides the sparse LU decomposition to solve the systems of the coupling, characterized by nontrivial sparsity patterns.

VII. Numerical Results

We run tests on meshes with different levels of refinement, given the geometry show in Fig. 1. As in [3], we use parameters $\sigma_{\mathrm{c}} = 3.5 \cdot 10^7 \, \mathrm{Sv\,m^{-1}}$, $\omega = 400\pi \, \mathrm{rad\,s^{-1}}$, $\mu_{\mathrm{c}} = \mu_{\mathrm{n}} = 4\pi \cdot 10^{-7} \, \mathrm{T\,m\,A^{-1}}$, and $I = 200 \, \mathrm{A}$.

Multipoles are uniformly disposed on a rectangular prism that lies completely inside Fig. 1 (i.e. outside the MMP domain of approximation). For each center we consider multipoles following (7) with $l = 0$, $m = 0$ and $l = 1$, $m = -1, 0, 1$. The total number of multipoles is proportional to the number of intersections of each mesh with Γ.

To validate our results, we first compute induced eddy currents I_3 and I_4, which are defined as surface integrals

$$I_i \coloneqq \int_{\Sigma_i} \mathbf{n} \cdot (\nabla \times \mathbf{H}_{\mathrm{c}}) \, \mathrm{d}S, \quad i = 3, 4, \tag{15}$$

where Σ_3 and Σ_4 are surfaces cutting Ω_{c} on each side of the hole of Fig. 1. For all meshes considered, the different coupling approaches return values similar to each other, with $|I_3| + |I_4|$ being very close to $I/2 = 100 \, \mathrm{A}$, as expected from the theory. This is shown in Figure 2.

We also compute the power loss of the conductor L_{c}, which is defined as the integral

$$L_{\mathrm{c}} \coloneqq \int_{\Omega_{\mathrm{c}}} \sigma_{\mathrm{c}} \, \|\mathbf{E}_{\mathrm{c}}\|^2 \, \mathrm{d}\mathbf{x} = \int_{\Omega_{\mathrm{c}}} \frac{1}{\sigma_{\mathrm{c}}} \, \|\nabla \times \mathbf{H}_{\mathrm{c}}\|^2 \, \mathrm{d}\mathbf{x}. \tag{16}$$

Again, Figure 3 shows that L_{c} stays constant throughout all our simulations, as expected.

Convergence tests for the relative $\mathbf{L}^2(\Omega^{\mathrm{f}})$-error of the **H**-field with respect to the most refined mesh are presented in Figure 4. All coupling approaches exhibit an algebraic convergence with a similar rate.

Finally, Figure 5 illustrates the magnitude of the **H**-field in Ω^{f} as seen from the front of Fig. 1 (along the XZ-plane), applying the DG-based coupling to the most refined mesh. Figures for the other coupling approaches are also very similar.

VIII. Conclusion

Compared to other hybrid methods, such as FEM coupled with the boundary element method, MMP presents the advantages of (1) a simpler assembly process, as there are no singular integrals, and (2) an exponentially convergent approximation error, given loose requirements on the positions of the multipoles. The latter point entails a small number of degrees of freedom for MMP, which, in the case of the DtN- and DG-based coupling approaches, can even be eliminated by
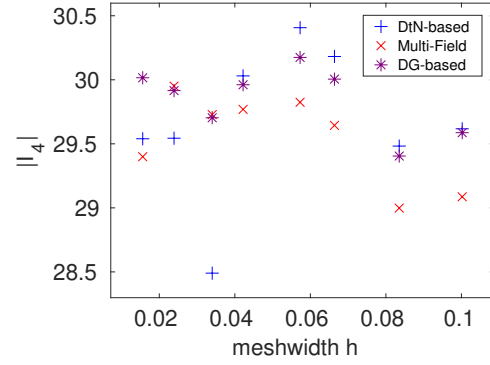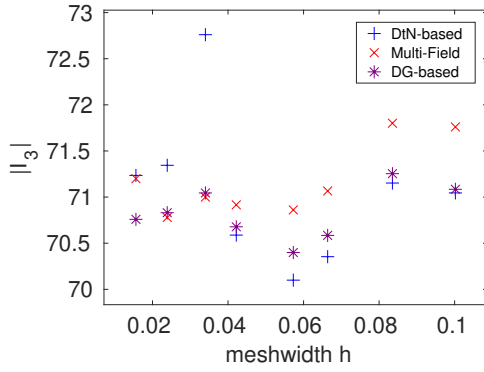
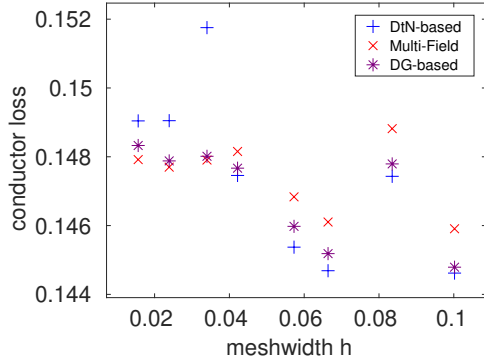Fig. 2. Computed $|I_3|$ and $|I_4|$ for different mesh refinements of the geometry in Fig. 1.

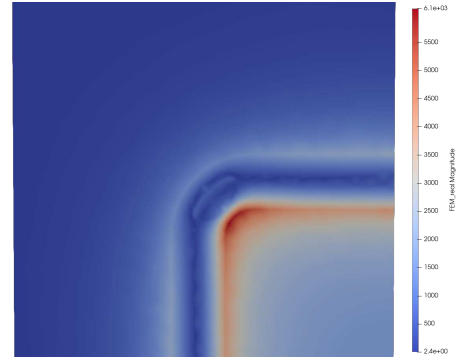Fig. 3. Computed L_c for different mesh refinements.

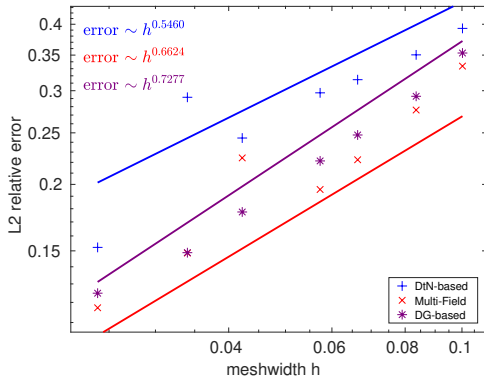Fig. 5. Computed $\|\mathbf{H}_f\|$ with DG-based coupling (XZ-plane).

Fig. 4. Convergence of $\mathbf{L}^2(\Omega^f)$-error w.r.t. most refined mesh.

computing the Schur complement of the final system. Using an iterative solver is also possible [9].

Among the three coupling approaches we present, we recommend the multi-field and DG-based coupling thanks to their reliability. The DtN-based coupling is the easiest to implement, but has (mild) stability issues.

REFERENCES

[1] C. J. Carpenter, "Comparison of alternative formulations of 3-dimensional magnetic-field and eddy-current problems at power frequencies," *Proceedings of the Institution of Electrical Engineers*, vol. 124, no. 11, pp. 1026–1034, November 1977.
[2] I. Mayergoyz, "A new approach to the calculation of three-dimensional skin effect problems," *IEEE Transactions on Magnetics*, vol. 19, no. 5, pp. 2198–2200, September 1983.
[3] J. Smajic, "Novel variant of the $\mathbf{H}$-ϕ field formulation for magnetostatic- and eddy current problems," *COMPEL*, submitted.
[4] C. Hafner, "OpenMaXwell," https://openmax.ethz.ch/, 2014, Institute of Electromagnetic Fields, ETH Zurich.
[5] J. Smajic, C. Hafner, and J. Leuthold, "Coupled FEM–MMP for computational electromagnetics," *IEEE Transactions on Magnetics*, vol. 52, no. 3, pp. 1–4, March 2016.
[6] D. Casati and R. Hiptmair, "Coupling finite elements and auxiliary sources," *Computers & Mathematics with Applications*, vol. 77, no. 6, pp. 1513–1526, March 2019. [Online]. Available: http://www.sciencedirect.com/science/article/pii/S089812211830511X
[7] D. Casati, R. Hiptmair, and J. Smajic, "Coupling finite elements and auxiliary sources for Maxwell's equations," *International Journal of Numerical Modelling: Electronic Networks, Devices and Fields*, forthcoming. [Online]. Available: https://onlinelibrary.wiley.com/doi/abs/10.1002/jnm.2534
[8] A. Bermúdez, R. Rodríguez, and P. Salgado, "Finite element methods for 3D eddy current problems in bounded domains subject to realistic boundary conditions. an application to metallurgical electrodes," *Archives of Computational Methods in Engineering*, vol. 12, no. 1, pp. 67–114, January 2005.
[9] D. Casati, L. Codecasa, R. Hiptmair, and F. Moro, "Trefftz co-chain calculus," *Progress in Electromagnetic Research*, submitted.
[10] C. Bernardi, Y. Maday, and F. Rapetti, "Basics and some applications of the mortar element method," *GAMM-Mitteilungen*, vol. 28, no. 2, pp. 97–123, May 2005.
[11] A. Popp, B. I. Wohlmuth, M. W. Gee, and W. A. Wall, "Dual quadratic mortar finite element methods for 3D finite deformation contact," *SIAM Journal on Scientific Computing*, vol. 34, no. 4, pp. B421–B446, 2012.
[12] D. N. Arnold, F. Brezzi, B. Cockburn, and L. D. Marini, "Unified analysis of Discontinuous Galerkin methods for elliptic problems," *SIAM Journal on Numerical Analysis*, vol. 39, no. 5, pp. 1749–1779, 2002.
[13] R. Stenberg, "Mortaring by a method of J.A. Nitsche," *Computational Mechanics: new trends and applications*, 1998.
[14] R. Casagrande and C. Winkelmann, "Hybrid Discontinuous finite elements for power devices (HyDi)," 2016, ABB Corporate Research Center.